Acta Crystallographica Section B
Structural Science
ISSN 0108-7681

Structure determination of forms I and II of phenobarbital from X-ray powder diffraction

Cyril Platteau,[a] Jacques Lefebvre,[a]* Stephanie Hemon,[a] Carsten Baehtz,[b] Florence Danede[b] and Dominique Prevost[a]

[a]Laboratoire de Dynamique et Structure des Matériaux Moléculaires (UMR CNRS 8024), UFR de Physique, Bâtiment P5, Université des Sciences et Technologies de Lille, 59655 Villeneuve d'Ascq CÉDEX, France, and [b]Materials Science, Darmstadt University of Technology, Petersenstrasse 23, 64287 Darmstadt, Germany

Correspondence e-mail: jacques.lefebvre@univ-lille1.fr

Received 9 July 2004
Accepted 26 November 2004

From pure powders of forms I and II of phenobarbital, X-ray diffraction patterns were recorded at room temperature. The starting crystal structural models were found by a Monte-Carlo simulated annealing method. The structures of the two forms were obtained through Rietveld refinements. Soft restraints were applied on bond lengths and bond angles, all H-atom positions were calculated. The cell of form I is monoclinic with the space group $P2_1/n$, $Z = 12$, $Z' = 3$. Form II has a triclinic cell, with the space group $P\bar{1}$, $Z = 6$, $Z' = 3$. For both forms, the crystal cohesion is achieved by networks of N—H···O hydrogen bonds along [101]. The broadening of the Bragg peak profiles is interpreted in terms of isotropic strain effects and anisotropic size effects.

1. Introduction

Phenobarbital ($C_{12}H_{12}O_3N_2$, also called 5-ethyl-5-phenylbarbituric acid or phenobarbitone) is a derivative of uracil and is physiologically used as a sedative hypnotic agent. The derivatives of the barbituric acid are known to show a high degree of polymorphism (see, for example, Cleverley & Williams, 1959; Brandstätter-Kuhnert & Aepkers, 1961) and phenobarbital has been found to exhibit the greatest number of polymorphs. Thirteen modifications have been characterized by IR spectroscopy, X-ray diffraction and differential scanning calorimetry (Mesley *et al.*, 1968). Among these 13 forms, 12 of them are anhydrous and many were only observed in binary mixed crystals containing other barbituric acids; the last form is a monohydrate. The reason for such a number of polymorphs is the possibility of a variety of intermolecular hydrogen-bonding schemes in the barbituric acid family (Craven *et al.*, 1969; Craven & Vizzini, 1971). Williams (1973) has reported cell parameters and space groups of five polymorphs. He solved the structure of the monohydrate form (form XIII; Williams, 1973) and one of the 12 anhydrous forms (form III; Williams, 1974) using single-crystal diffraction. The structure of the complex of phenobarbital with theophylline has also been determined (Nakao *et al.*, 1977). To our knowledge, no additional structure of any phenobarbital phase has been determined.

Phenobarbital is commercially available as form II according to Mesley *et al.* (1968). Taking into account the possibility that the form changes when dissolved in a solvent and recrystallized to obtain single crystals, our first idea was to use this commercial chemical to determine the crystal structure of this form from X-ray powder diffraction measurements. Experiments were performed with the synchrotron radiation source of the HASYLAB (DESY, Hamburg, Germany). Unfortunately, the commercial powder contains an unidentified impurity. A thermal and chemical treatment was

Table 1
Bond lengths (Å) and angles (°) used to build the molecule for the program *FOX* and as input for the soft constraints.

Mean values and r.m.s. deviations are found after Rietveld refinements for the two forms. The indexes 'pyr', 'et' and 'ph' represent the pyrimidine ring, ethyl group and phenyl ring, respectively. Atom C5 of the pyrimidine ring links the ethyl group and the phenyl ring. The r.m.s. deviation σ is defined by: $\sigma = \sigma = \left[\sum_{i=1}^{N}(V_i - V_{\rm mean})^2/N\right]^{1/2}$, where N is the number of observations.

	Input values	Form I	Form II
$C_{pyr}-N_{pyr}$	1.370	1.376 (8)	1.372 (10)
$C_{pyr}-C_{pyr}$, $C_{et}-C_{et}$	1.522	1.530 (5)	1.528 (10)
$C_{pyr}=O$	1.215	1.214 (5)	1.221 (7)
C_5-C_{et}, C_5-C_{ph}	1.545	1.548 (6)	1.547 (7)
$C_{ph}-C_{ph}$	1.395	1.394 (8)	1.393 (6)
$N_{pyr}-C_{pyr}-N_{pyr}$	116.5	115.4 (4.2)	115.9 (3.0)
$C_{pyr}-N_{pyr}-C_{pyr}$	125.5	127.1 (3.8)	125.4 (3.0)
$N_{pyr}-C_{pyr}-C_{pyr}$	117.0	116.1 (2.6)	118.5 (4.5)
$C_{pyr}-C_5-C_{pyr}$	111.0	114.3 (1.6)	111.6 (5.8)
$C_{pyr}-C_5-C_{et}$	107.6	108.7 (1.8)	107.7 (3.6)
$C_5-C_{et}-C_{et}$	114.5	112.3 (4.9)	113.7 (2.2)
$C_{pyr}-C_5-C_{ph}$	110.2	108.0 (3.0)	109.5 (4.2)
$C_5-C_{ph}-C_{ph}$	120.0	122.1 (3.5)	120.4 (8.0)
$C_{ph}-C_{ph}-C_{ph}$	120.0	119.6 (4.4)	119.7 (3.6)

necessary to remove this impurity and pure crystallized powders of forms I and II were obtained.

The aim of this paper is to explain the determination of the crystal structures of forms I and II of phenobarbital from X-ray powder diffraction experiments. The *ab initio* structure determination was performed with a simulated-annealing method in order to obtain a starting model, followed by Rietveld refinements using soft constraints on bond lengths and angles.

2. Data collection

2.1. Form II

Phenobarbital powder for this experiment came from Aldrich Chemical Company with a purity rate of 99%. A first X-ray pattern of this powder was collected at room temperature on the B2 diffractometer located on the synchrotron radiation source of HASYLAB (DESY, Hamburg, Germany). The wavelength was 1.1199 (1) Å and the 2θ range ran from 4.5 to 40° with a step width of 0.003°. A scintillation counter with a Ge(111) analysing crystal was used in order to obtain high resolution. Powder was introduced into a Lindemann glass capillary of 1 mm diameter.

To determine the cell, the position of the Bragg peaks between 4.5 and 18°, 2θ, was extracted with the program *WINPLOTR* (Roisnel & Rodriguez-Carvajal, 2002). The 20 most intense reflections were introduced into *TREOR* (Werner *et al.*, 1985) and a triclinic cell was found. To refine the lattice parameters and the parameters of the width of the reflections, the Profile Matching option of *FullProf* (Rodriguez-Carvajal, 2001) was used. The lattice parameters of the triclinic cell are: a = 10.737, b = 23.542, c = 6.787 Å, α = 90.98, β = 94.48, γ = 88.13°, V = 1709.2 Å^3. With the usual rule of 18 Å^3 per non-H atom (Kempster & Lipson, 1972), this volume corresponds to Z = 6 molecules per unit cell. These parameters for form II of phenobarbital are in agreement with those found by Williams (1973).[1] Nevertheless, some reflections with a low intensity were not indexed. These reflections are due to an impurity contained in the commercial powder and it was not possible to identify it.

If the sample is a mixture of two phases, determination of the structure of one of those phases from an X-ray powder pattern requires that the structure of the other phase be known. This is not the present case and to obtain a pure compound of form II, commercial powder was dissolved in hot methanol with boneblack. Then the solution was heat-filtered and phenobarbital precipitated during the cooling.

A second experiment was performed on a laboratory diffractometer equipped with an INEL curved sensitive detector CPS 120 composed of 4096 channels, allowing X-ray diffraction in a 2θ range of about 120° to be recorded simultaneously. The incident beam was monochromated with a bent quartz crystal which selects the $K\alpha_1$ wavelength of a Cu X-ray tube (λ = 1.54056 Å). Powder was introduced into a Lindemann glass capillary of 0.7 mm in diameter. The correspondence between the channel number and the 2θ angle was determined by a preliminary X-ray diffraction pattern of cubic $Na_2Ca_2Al_2F_{14}$ (NAC; Evain *et al.*, 1993) with a cubic spline interpolation between the Bragg peaks of NAC. This pattern was also used to determine the parameters of the experimental resolution. The profile of the peaks is correctly interpreted by pseudo-Voigt functions. The Gaussian component has a θ dependence according to Caglioti's law (Caglioti *et al.*, 1958); the θ dependence of the Lorentzian component is

$$\Gamma_L = X_{\rm ins}\tan\theta + (Y_{ins}/\cos\theta)$$

with $U_{\rm ins}$ = 0.01858, $V_{\rm ins}$ = −0.01949, $W_{\rm ins}$ = 0.01208 deg^2, $X_{\rm ins}$ = 0.01814 and $Y_{\rm ins}$ = 0.1882°. After the thermal treatment, the compound was pure and the same cell as previously was found.

2.2. Form I

Form I of phenobarbital was obtained by heating commercial powder at 438 K over 24 h and under low pressure (10^{-2} to 10^{-3} mm Hg; Mesley *et al.*, 1968). Because of the possibility of reversion to form II, the X-ray pattern of this form was recorded just after this thermal treatment.

The X-ray pattern was recorded on the laboratory diffractometer with the same set-up as previously used. The space group $P2_1/n$ and the lattice parameters given by Williams (1973) for form I were input into the program *FullProf* (Rodriguez-Carvajal, 2001) and Le Bail refinements confirm the results of Williams. As a result of these refinements, the parameters of the monoclinic cell are: a = 10.692, b = 47.116, c = 6.801 Å, β = 94.19°, V = 3417 Å^3 (with respect to the parameters of Williams, the same lattice transformation as for form II was carried out). The volume was twice that of form II and the number of molecules per cell is Z = 12.

[1] The correspondence between the Williams parameters and the parameters of this paper is as follows: $a = c_W$, $b = -b_W$, $c = a_W$.

Table 2
Agreement factors for isotropic and anisotropic size and strain effects of the Le Bail refinements for X-ray diffraction patterns on forms I and II of phenobarbital.

	Isotropic size Isotropic strain	Anisotropic size Isotropic strain	Isotropic size Anisotropic strain	Anisotropic size Anisotropic strain
(*a*) Form I				
R_p	0.0599	0.0583	0.0607	0.0582
R_{wp}	0.0695	0.0674	0.0690	0.0669
R_{exp}	0.0164	0.0166	0.0165	0.0162
χ^2	17.9	16.5	17.5	17.0
Average size (Å)	1107 (1)	828 (78)	1186 (5)	945 (113)
Average strain ($\times 10^{-4}$)	7.58 (3)	10.24 (2)	6.12 (2.28)	4.23 (2.74)
(*b*) Form II				
R_p	0.0729	0.0669	0.0724	0.0678
R_{wp}	0.0801	0.0730	0.0797	0.0729
R_{exp}	0.0185	0.0185	0.0184	0.0185
χ^2	18.8	15.6	18.7	15.6
Average size (Å)	830 (2)	792 (88)	867 (3)	816 (119)
Average strain ($\times 10^{-4}$)	10.49 (3)	9.82 (2)	7.78 (2.89)	6.76 (2.80)

3. Structure solution and refinement

In order to obtain a starting structural model of form II in spite of the presence of an impurity, Monte-Carlo simulated annealing calculations were performed with the 'parallel tempering' algorithm of the program *FOX* (Favre-Nicolin & Cerny, 2002). The simulated pattern was compared with the pattern recorded on the diffractometer B2 with a 2θ range running from 4.5 to 30°. Lattice and profile parameters, and zero-point and interpolated backgrounds calculated with Le Bail refinements were introduced into the program. The chosen space group was $P\bar{1}$ with $Z' = 3$ molecules in the asymmetric unit, which were used in *FOX* without taking the H atoms into account. The average bond lengths and angles of forms III and XIII were used to build these molecules and are reported in Table 1; the pyrimidine and phenyl rings are taken as planar. During the simulated annealing calculations, each molecule could translate and rotate randomly; torsion angles between the pyrimidine and phenyl rings on one hand and between the pyrimidine ring and the ethyl group on the other hand could also change. For the three molecules of the asymmetric unit, there are 30 degrees of freedom. After *ca* 20 million trials, the agreement *FOX* factor *wR* was 0.191: the final configuration with the triclinic space group $P\bar{1}$ could constitute a starting structural model. In particular, the lowest distance between atoms of neighbouring molecules was 2.36 Å.

The program *FOX* was also used for form I with the simulated pattern compared with the experimental pattern obtained using the diffractometer equipped with a CPS120 curved detector for 2θ in the range 7–50°. The space group was $P2_1/n$ with $Z' = 3$ molecules in the asymmetric unit. The same molecules as before were introduced and there were also 30 degrees of freedom during the simulated annealing calculations. After 15 millions trials, the agreement factor fell to 0.125 and the obtained configuration is introduced as the starting structural model for this form.

For the two forms, atomic coordinates of non-H atoms found by *FOX* were introduced into the program *FullProf* (Rodriguez-Carvajal, 2001) using the patterns recorded with the laboratory diffractometer. The coordinates of the H atoms were determined geometrically with the program *DEBVIN* (Brückner & Immirzi, 1997). The two H atoms of the pyrimidine rings were in the C—N—C plane, in the external bisector of the C—N—C angle with an N—H length of 1.03 Å. The same method was used for H atoms of the phenyl rings with a C—H length of 1.01 Å. For the ethyls, the two H atoms of the CH_2 groups were such that the C—C—C and H—C—H planes were perpendicular with the two H atoms symmetrically located with respect to the C—C—C plane with a H—C—H angle of 108°. For the three H atoms of the CH_3 groups, the C—C bond constituted a local threefold axis for the H atoms with

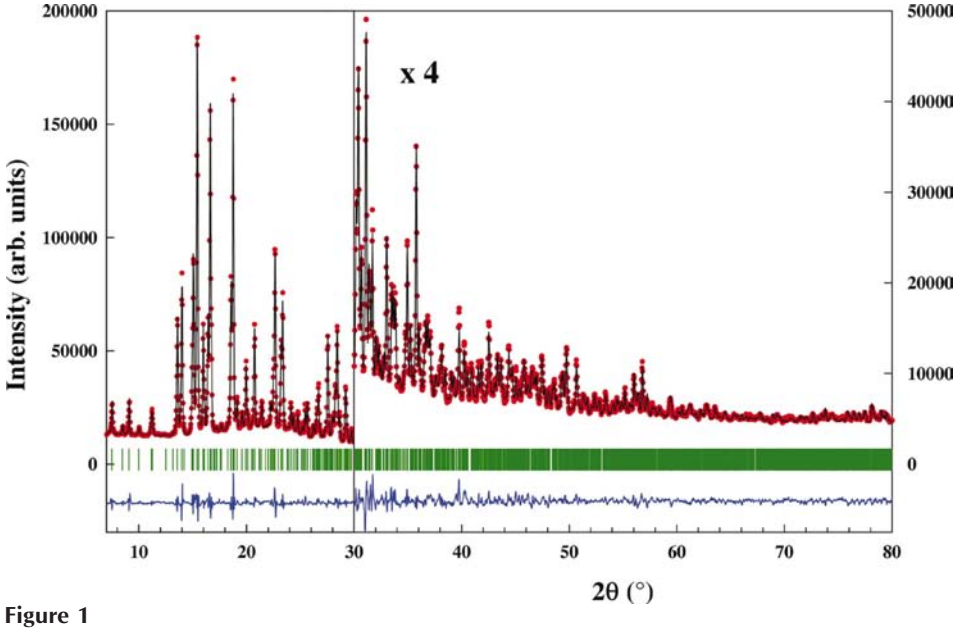

Figure 1
Final Rietveld plot of form I of phenobarbital. Observed data points are indicated by dots, the best fit profile (upper trace) and the difference pattern (lower trace) are solid lines. The vertical bars correspond to the positions of the Bragg peaks.

Table 3
Crystallographic data for forms (I) and (II) of phenobarbital.

	Form I	Form II
Formula	$C_{12}H_{12}O_3N_2$	$C_{12}H_{12}O_3N_2$
M_r	232.24	232.24
Crystal system	Monoclinic	Triclinic
Space group	$P2_1/n$	$P\bar{1}$
a (Å)	10.6907 (2)	10.7313 (3)
b (Å)	47.125 (1)	23.5112 (7)
c (Å)	6.8002 (2)	6.7831 (2)
α (°)	90	90.969 (1)
β (°)	94.185 (1)	94.476 (1)
γ (°)	90	88.153 (1)
V (Å^3)	3416.8 (1)	1705.1 (1)
Z	12	6
D_c (g cm^{-3})	1.354	1.357
F(000)	1464	732
μ (mm^{-1})	0.824	0.825
2θ range (°)	7–80	7–80
Step size (° 2θ)	0.029	0.029
Wavelength (Å)	1.54056	1.54056
No. of profile data steps	2517	2517
No. of contributing reflections	2077	2071
No. of structural variables	158	158
No. of profile parameters	18	17
No. of background points refined	29	29
No. of bond length constraints	54	54
No. of bond angle constraints	63	63
R_p	0.0818	0.0751
R_{wp}	0.0855	0.0801
R_{exp}	0.0182	0.0189
χ^2	22.1	18.0
R_B	0.0282	0.0241
R_F	0.0419	0.0332

C—C—H bond angles of 108° and the C—C—C—H torsion angles adjusted with *DEBVIN*. The C—H bond length was 1.01 Å for the CH_2 and CH_3 groups. During the Rietveld refinements with *FullProf* (Rodriguez-Carvajal, 2001), the H atoms underwent the same shifts as their linked atom. Nevertheless, because of the possibility of the rotation or distortion of the molecules, the previous procedure was repeated several times.

The 2θ range used in the Rietveld refinements runs from 7 to 80° for the two forms. The coordinates of the 51 independent non-H atoms were fitted, but soft constraints on bond lengths and angles were introduced in order to reduce the number of free parameters. The values of the constraints are those of the lengths and angles used previously in the program *FOX* (see Table 1), with a standard error of 0.01 Å for all bond lengths and 1° for all bond angles. An isotropic global temperature factor was introduced for each of the three molecules of the asymmetric unit. Intensities were corrected for absorption effects for a cylindrical sample with $\mu R = 0.28$.

The peak profiles were adjusted with pseudo-Voigt functions using the Thompson–Cox–Hastings formalism (Thompson *et al.*, 1987), which can take into account the experimental resolution and the broadening due to size and strain effects. These two effects can be isotropic or anisotropic, and the analytical expression of the HWHM of the Gaussian and Lorentzian components of the pseudo-Voigt function is given elsewhere (Rodriguez-Carvajal & Roisnel, 2004). Le Bail refinements have been carried out for forms I and II, for 2θ in the range 7–60° and with four possibilities for the isotropic or (and) anisotropic effects. Table 2 reports, for the two forms, the Rietveld agreement factors as well as the average sizes and strains. From the 'all isotropic' case and for the two forms, a distinct improvement in the R_{wp} factor is seen when the size effects are anisotropic and for all cases, there is only a small decrease of R_{wp} when anisotropic strain effects are introduced into the pseudo-Voigt profiles. Following these calculations, in the following and for the two forms refinements were carried out with isotropic strain and anisotropic size effects. The number of profile parameters is 11 for the monoclinic form I and 8 for the triclinic form II.

The asymmetry of the peak profile is taken into account with the two first parameters of the Bérar & Baldinozzi (1993) function. The effects of the preferred orientations are calculated according to the March (1932) and Dollase (1986) formalism with only the G_1 parameter refined. For the two forms, 29 points of background are regularly distributed between 7 and 80°, 2θ, and a linear interpolation is made between two successive points.

Finally, there are 205 adjustable parameters for form I and 204 for form II with 117 soft constraints in both cases. The final conventional agreement factors for form I are: $R_p = 0.082$, $R_{wp} = 0.086$, $R_{exp} = 0.018$, $\chi^2 = 22.1$, $R_B = 0.028$ and $R_F = 0.042$. The root mean-square (r.m.s.) deviations to the assigned values are 0.009 Å for the bond lengths and 3.9° for the bond angles for the soft constraints. The plot of the X-ray pattern of form I is given Fig. 1. For form II, the corresponding values are: $R_p = 0.075$, $R_{wp} = 0.080$, $R_{exp} = 0.019$, $\chi^2 = 18.0$, $R_B = 0.024$ and $R_F = 0.033$; the r.m.s. deviations to the assigned values for the soft constraints are 0.009 Å and 4.2° for the bond lengths and angles, respectively. Fig. 2 shows the plot of the X-ray pattern of form II. Crystallographic data, profile and structural parameters of the two forms of phenobarbital are reported in Tables 3 and 4, respectively, and in the supplementary data.[2] The molecular structure, drawn with *ORTEP*3 (Farrugia, 1997), and the atom-numbering are shown in Fig. 3. Figs. 4 and 5 report the projection of the cell content in the *ab* plane for forms I and II, respectively.

4. Discussion

Table 1 gives the mean values with their r.m.s. deviations for the different types of bond lengths and angles. The values of the mean bond lengths are closed to those of the soft constraints which are also the mean values of forms III and XIII of phenobarbital. As a consequence of the low discrepancies in the bond length values, the r.m.s. deviations are in the range 0.005–0.010 Å and they are smaller than the standard deviations given by the Rietveld refinements, which vary

[2] Supplementary data for this paper are available from the IUCr electronic archives (Reference: LC5012). Services for accessing these data are described at the back of the journal.

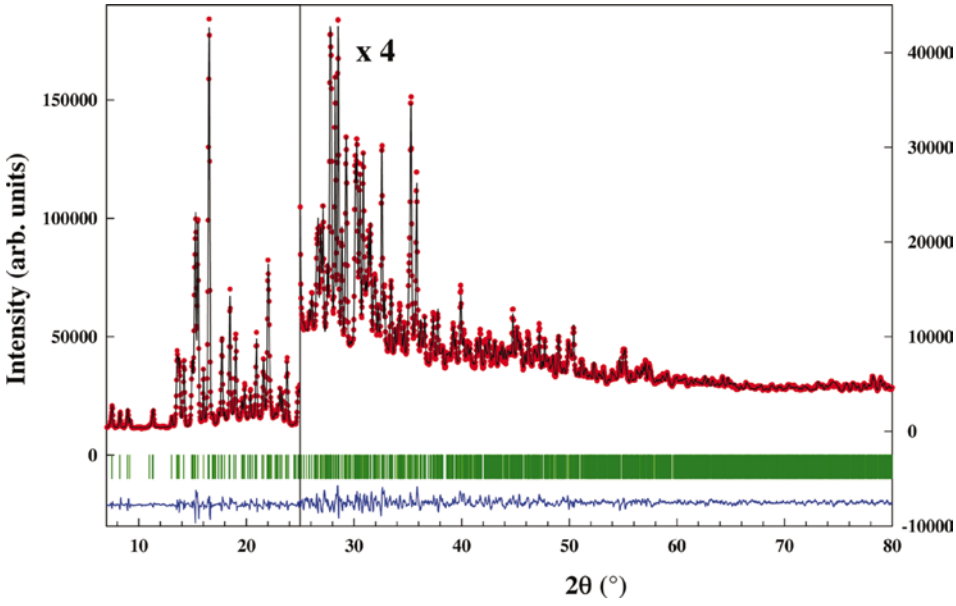

Figure 2
Final Rietveld plot of form II of phenobarbital. See Fig. 1 for details.

between 0.013 and 0.029 Å. The mean bond lengths are also closed to the soft constraints, but large r.m.s. deviations are observed. In particular, it is the $C_5-C_{ph}-C_{ph}$ angles of form II which deviate significantly from 120°. For example, for molecule 2 of form II, C*b*5—C*b*9—C*b*10 and C*b*5—C*b*9—C*b*14 equal 131.7 and 110.9°, respectively. An explanation of such a difference is given in the following.

The unit-cell volume of form I is twice that of form II, because of the lattice parameter *b* doubling, while the other parameters remain virtually equal with, in particular, values close to 90° for the triclinic angles α and γ for form II. The unit cells of these two forms are completely different to those of forms III and XIII (Williams, 1973).

The molecular packing of form I can be explained as follows (Fig. 6): in the *ac* plane, near $y = 0.0$ (Fig. 6*a*), there are two molecules (molecule 2) generated; one related to the other by the inversion centre. The two other molecules (2) are also in an *ac* plane at $y \simeq 0.5$ (Fig. 6*c*); they are obtained from those in the *ac* plane at $y \simeq 0.0$ by the twofold screw axis. Two molecules (1) are in the *ac* plane located at $y \simeq 0.25$ (Fig. 6*b*) and they are connected with the glide plane. The twofold screw axis generates the two other molecules (1) in the *ac* plane at $y \simeq 0.75$ (Fig. 6*d*). Molecules (3) are inserted between the planes of molecules (1) and (2). The crystalline cohesion energy is assumed by the N—H···O hydrogen bonds (Table 5). For the three molecules of the asymmetric unit, all six N atoms are donors, O*a*4 and O*a*6 are twice acceptors, O*b*4 and O*b*6 are once acceptors, and O*i*2, O*c*4 and O*c*6 atoms are not involved in hydrogen bonding. Every molecule (2) is linked by two hydrogen bonds to each of the two molecules (2) located in the same *ac* plane and on either side of it. Infinite chains of molecules (2) are then formed in the [101] direction. Every molecule (1) is also linked by two hydrogen bonds to each of the two neighbouring molecules (1) in the same *ac* plane and molecules (1) also form infinite chains along [101]. The two N atoms of molecules (3) are involved in hydrogen bonds with O*a*4 and O*a*6 atoms of two different molecules (1). For these hydrogen bonds, it is also noted that the N···O distances between molecules (1) and molecules (2) are smaller (2.887–2.965 Å, mean 2.922 Å) than those between molecules (3) and molecules (1) where the mean value is 3.000 Å.

Table 5(*a*) also reports the interatomic distances between non-H atoms of the neighbouring molecules which are shorter than 3.5 Å. Between molecules (1), there is only one contact along **c**. For molecules (2) there are contacts between molecules already linked by hydrogen bonds, but short interatomic distances are also observed between molecule (2) of the asymmetric unit and one located at $(-x, -y, -z+1)$. These interactions between atoms of the two molecules are, approximately, in the $[\bar{1}01]$ direction. Molecules (3) inserted between planes of molecules (1) and (2) have several interatomic contacts with the neighbouring molecules in these planes. Molecule (3) of the asymmetric unit has nine atom–atom distances shorter than 3.5 Å with five molecules (1), all located in the *ac* plane near $y = 0.25$. Among these five molecules (1), the two linked by hydrogen bonds to molecule (3) are included. Similarly, with molecules (2) of the (*ac*) plane at $y \simeq 0.0$, there are five interatomic distances shorter than 3.5 Å with molecule (3). These five short distances are from four different molecules of (2). The interactions between molecules (3) and planes of molecules (1) and (2) supply the

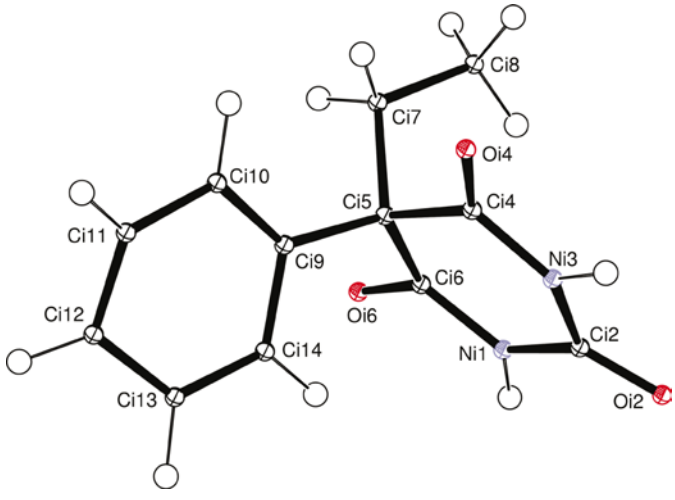

Figure 3
Atomic numbering and structure of a molecule of phenobarbital.

Table 4
Profile and structural parameters for forms I and II of phenobarbital obtained after Rietveld refinements with *FullProf*.

	Form I	Form II
U_{ST}	−0.005 (2)	0.010 (3)
G_{SZ}	0.0034 (2)	−0.0004 (2)
C_{00}	0.354 (27)	0.935 (28)
C_{20}	−0.066(24)	−0.319 (22)
C_{21+}	–	−0.201 (16)
C_{21-}	–	−0.051 (16)
C_{22+}	0.514 (39)	−0.578 (26)
C_{22-}	0.188 (18)	−0.140 (23)
C_{40}	0.025 (29)	–
C_{42+}	0.120 (17)	–
C_{42-}	0.193 (21)	–
C_{44+}	0.138 (39)	–
C_{44-}	−0.237 (19)	–
$Asym_1$	−0.026 (5)	0.001 (5)
$Asym_2$	0.020 (1)	0.015 (1)
Preferred orientations	[010]	[010]
G_1	1.083 (5)	1.118 (6)
B_{iso} (Å^2), molecule (1)	1.96 (18)	0.56 (18)
B_{iso} (Å^2), molecule (2)	1.02 (16)	1.56 (22)
B_{iso} (Å^2), molecule (3)	2.91 (20)	3.87 (21)

crystalline cohesion along the twofold screw axis. It is also noteworthy that for all short interatomic distances between neighbouring molecules, an O atom is always involved with a C, N or O atom.

The molecular packing of the triclinic form II of phenobarbital is similar to form I (Fig. 7). In the *ac* plane at $y \simeq 0.0$ (Fig. 7*a*), the two molecules (2) of the unit cell are arranged as form I with the same N—H···O hydrogen bonds (Table 5). These hydrogen bonds form infinite chains parallel to the [101] direction. The two molecules (1) are also located in an *ac* plane at $y \simeq 0.5$ (Fig. 7*b*), but unlike form I, they are connected by an inversion centre. Nevertheless, every N atom of this molecule is a donor for the N—H···O bonds with O*a*4 and O*a*6 of molecules (1) located in the same plane. Between two neighbouring molecules (1) there two hydrogen bonds and they also form infinite chains along [101]. Molecules (3) are inserted between planes of molecules (1) and (2). The two N atoms of molecules (3) are also involved in hydrogen bonds with O*a*4 and O*a*6 of two different molecules (1). For hydrogen bonds between molecules (1) and (2), N···O distances run from 2.871 to 2.975 Å with a mean value of 2.932 Å. As for form I, the N···O distances of the hydrogen bonds between molecules (3) and (1) are higher with a mean value of 3.070 Å.

In form II the network of the short interatomic distances between neighbouring molecules is almost identical to the network in form I (Table 5*b*) with one contact along *c* between molecules (1) and, for molecules (2), the non-hydrogen-bonded molecule located at $(-x, -y, -z+1)$ also has short contact distances with molecule (2) of the asymmetric unit. Molecule (3) of the asymmetric unit presents short interatomic distances with five molecules (1) and three molecules (2) located in *ac* planes at $y \simeq 0.5$ and $y \simeq 0.0$, respectively. The shorter distance, 3.14 Å, is observed between O*c*6 and C*b*11^{xvi} (see Table 5 for symmetry code). It has been seen that the two angles C*b*5—C*b*9—C*b*10 and C*b*5—C*b*9—C*b*14 differ from the ideal value

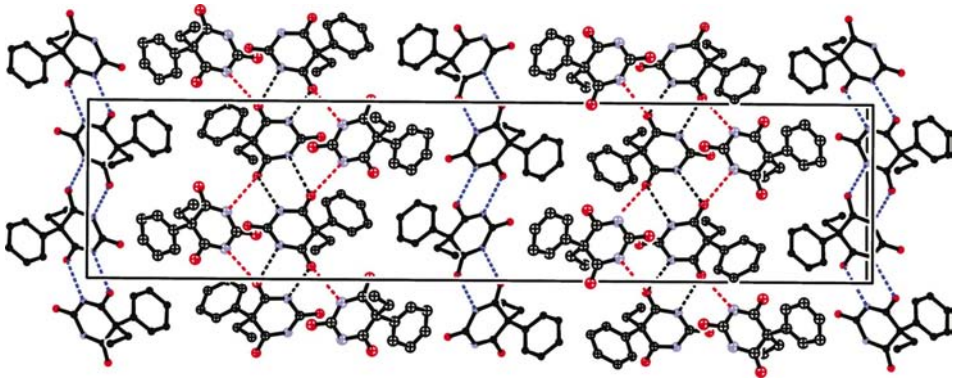

Figure 4
The unit cell of form I of phenobarbital projected in the *ab* plane. Black dashed lines show the hydrogen-bonding network between molecules (1) of the asymmetric unit; blue dashed lines correspond to the hydrogen-bonding networks between molecules (2); red dashed lines are the hydrogen bonds between molecules (3) and (1) of the asymmetric unit.

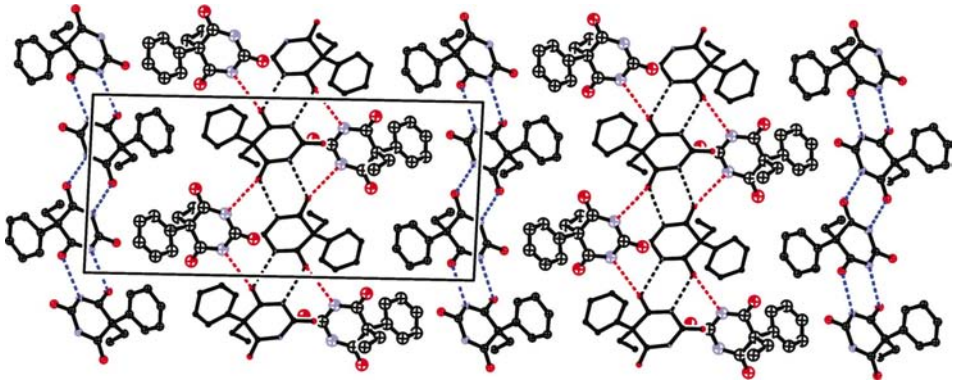

Figure 5
The unit cell of form II of phenobarbital projected in the *ab* plane. See Fig. 4 for details.

of 120°. In fact, the value of 131.7° for C*b*5—C*b*9—C*b*10 allows the distance between O*c*6 and the phenyl ring of a neighbouring molecule (2) to increase.

Forms I and II of phenobarbital show several similarities with form III (Williams, 1974): the crystal cohesion is provided by hydrogen-bond networks and the O*i*2 atoms are never involved in hydrogen-bond formation. Two of the three molecules of the asymmetric unit, linked by hydrogen bonds, form parallel infinite chains. Molecules (1) and (2) are located in planes. The pyrimidine rings of molecules 1 and 3 are face to face and they generate hydrophilic sheets parallel to the *ac* plane. Unlike form III, the pyrimidine rings of molecules (2) are, for the two forms studied, in front of the phenyl rings of molecules (3) and there are no lipophilic sheets in these two forms.

The program *FullProf* (Rodriguez-Carvajal, 2001) finds, for the two studied forms of phenobarbital, a preferred orientation along [010] with a calculated parameter G_1 of the March (1932) and Dollase (1986) function greater than 1, the G_2 parameter being taken as zero. These values of G_1, for a Debye–Scherrer geometry of the diffractometer, correspond to a platy habit of the crystallites.

For the two forms, the broadening of the Bragg peaks due to strain effects is taken to be isotropic. The calculated average values $\Delta d/d$ of the strain are small in both cases: 3.35×10^{-4} for form I and 4.72×10^{-4} for form II. These low values indicate few defects in the lattices. On the contrary, the size effects on the peak broadening are anisotropic, and Figs. 8 and 9 show the average shape of the crystallites in the monoclinic plane for form (I) and in the $(a,a \times b^*)$ plane for form II, respectively. For form II, the values of the triclinic angles α and γ are close to 90°, the $a \times b^*$ direction can be bounded up with the c^* direction and the $a \times b^*$ plane is close to the *ac* plane.

For form I, the calculated average diameter of the crystallites is 1040 Å with a minimal value of 690 Å along *b* and a maximal value of 1410 Å in the [232]* direction. The effect of the preferred orientations was to predict a platy-habit shape perpendicular to *b* for the crystallites and the previous values confirm this conclusion. In the *ac* plane the direction of the largest calculated dimension of the crystallite makes a φ angle of 30° with the lattice parameter *a* (see Fig. 8). This direction is also, approximately, the direction of the hydrogen bonds between molecules (1) and molecules (2), which are the strongest intermolecular interactions: hydrogen bonds are along [101] and the angle between this direction and *a* equals 33.6°.

The average diameter of the crystallites of form II equals 1085 Å with a minimal value of 580 Å along

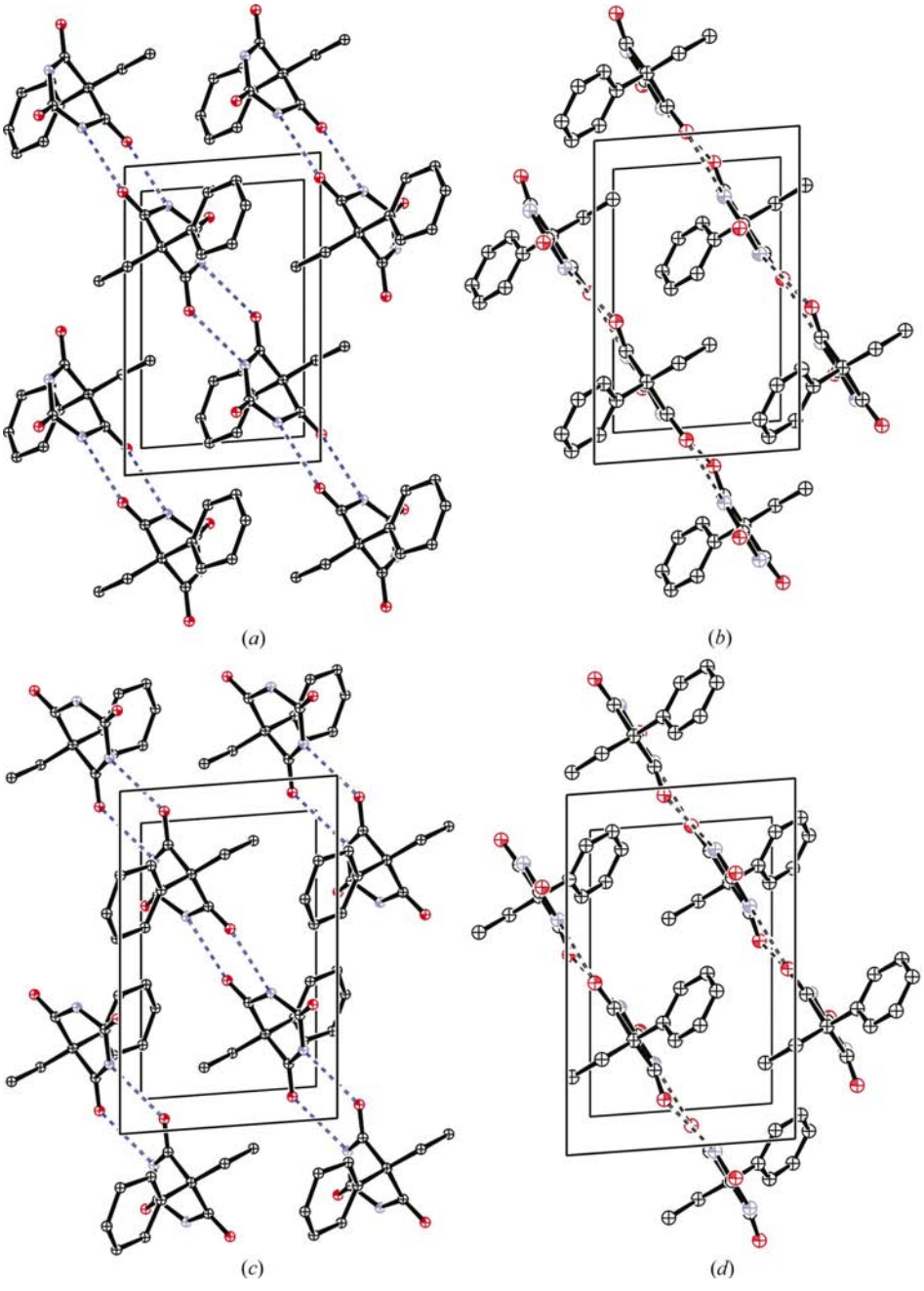

Figure 6
A slice of the structure of form I of phenobarbital projected in the *ac* plane: (*a*) $y \simeq 0.0$: molecule (2); (*b*) $y \simeq 0.25$: molecule (1); (*c*) $y \simeq 0.5$: molecules (2); (*d*) $y \simeq 0.75$: molecules (1). See Fig. 4 for details.

b^* and a maximal value of 2030 Å along [412]*. These values are also in agreement with the result of the preferred orientation. As the anisotropy is more important for form II than for form I, the calculated parameter G_1 for form II (G_1 = 1.118) is greater than that of form I (G_1 = 1.083). Fig. 9 shows that in the ($aa \times b^*$) plane the crystallites have an ellipsoid shape with its long axis making an angle of 42° with a. The long axis of this ellipsoid is close to the direction of most of the hydrogen bonds of form II which are along [101], the angle between this direction and a being equal to 33.5°.

This work was supported by the IHP-Contract HPRI-CT-1999-00040/2001-00140 of the European Commission.

References

Bérar, J. F. & Baldinozzi, G. (1993). *J. Appl. Cryst.* **26**, 128–129.
Brandstätter-Kuhnert, M. & Aepkers, M. (1961). *Mikroskopie*, **16**, 189–197.

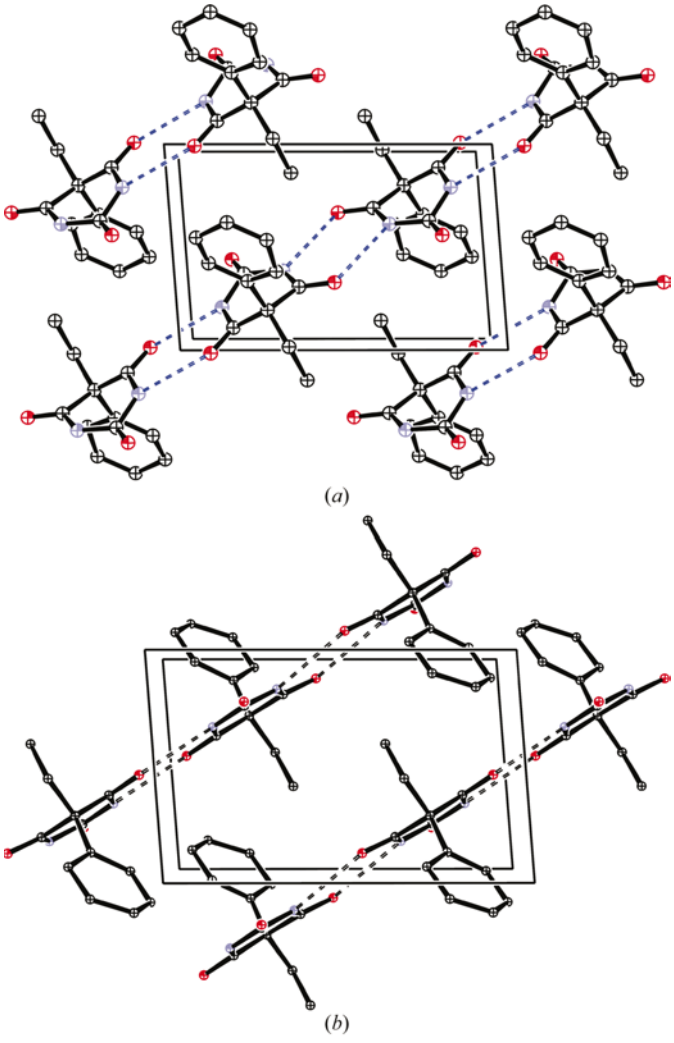

Figure 7
A slice of the structure of form II of phenobarbital projected in the *ac* plane: (*a*) $y \simeq 0.0$: molecule (2); (*b*) $y \simeq 0.5$: molecule (1). See Fig. 4 for details.

Table 5
Hydrogen-bonding geometry (Å, °) and shorter interatomic distances (Å) for forms I and II of phenobarbital.

D—H···A	D—H	H···A	D···A	D—H···A
(*a*) Form I				
N*a*1—H*a*1···O*a*4^{i}	1.030	1.917 (20)	2.931 (20)	167.5 (14)
N*a*3—H*a*3···O*a*6^{ii}	1.031	2.016 (21)	2.965 (20)	151.6 (13)
N*b*1—H*b*1···O*b*6^{iii}	1.030	1.958 (19)	2.906 (19)	151.6 (14)
N*b*3—H*b*3···O*b*4^{iv}	1.029	1.887 (19)	2.887 (19)	162.9 (14)
N*c*1—H*c*1···O*a*4^{i}	1.031	2.055 (22)	2.995 (21)	150.4 (14)
N*c*3—H*c*3···O*a*6^{v}	1.029	1.989 (19)	3.006 (19)	168.9 (13)
O*a*4···C*a*13^{vi}	3.37 (2)		O*c*2···C*a*2^{vii}	3.23 (3)
			O*c*2···N*a*3^{vii}	3.34 (2)
O*b*2···C*b*10^{viii}	3.42 (2)		O*c*2···O*a*2^{vii}	3.32 (3)
O*b*2···C*b*11^{viii}	3.31 (2)		O*c*4···C*a*10^{v}	3.34 (2)
O*b*4···O*b*4^{iv}	3.43 (2)		O*c*4···C*a*7^{v}	3.44 (2)
O*b*6···C*b*6^{iii}	3.49 (2)		O*c*6···C*a*12^{ix}	3.23 (2)
O*b*6···O*b*6^{iii}	3.31 (2)		O*c*4···C*b*13^{iv}	3.23 (2)
			O*c*6···C*b*11^{viii}	3.35 (2)
N*c*1···O*a*2	3.24 (2)		O*c*6···C*b*12^{viii}	3.29 (2)
N*c*1···C*a*14^{i}	3.35 (2)		C*c*12···O*b*2^{vii}	3.36 (2)
C*c*2···O*a*2	3.39 (3)		C*c*13···O*b*6^{iii}	3.50 (2)

D—H···A	D—H	H···A	D···A	D—H···A
N*a*1—H*a*1···O*a*6^{x}	1.030	1.979 (19)	2.964 (19)	159.2 (13)
N*a*3—H*a*3···O*a*4^{xi}	1.030	1.951 (20)	2.975 (20)	172.6 (15)
N*b*1—H*b*1···O*b*6^{xii}	1.030	1.874 (21)	2.871 (20)	161.8 (14)
N*b*3—H*b*3···O*b*4^{xiii}	1.030	1.921 (20)	2.916 (20)	161.6 (16)
N*c*1—H*c*1···O*a*6^{x}	1.030	2.041 (19)	3.049 (19)	165.5 (13)
N*c*3—H*c*3···O*a*4^{v}	1.030	2.103 (21)	3.092 (21)	160.3 (14)
O*a*6···C*a*13^{xv}	3.48 (2)		O*c*2···N*a*3^{xv}	3.44 (2)
			O*c*2···O*a*2^{xv}	3.17 (2)
O*b*2···C*b*10^{xvi}	3.41 (2)		O*c*2···O*a*6^{x}	3.43 (2)
O*b*2···C*b*11^{xvi}	3.39 (2)		O*c*4···C*a*10^{xiv}	3.25 (2)
O*b*4···O*b*4^{xiii}	3.38 (2)		O*c*6···C*a*12^{xvii}	3.22 (2)
			C*c*8···O*a*2	3.49 (2)
N*c*1···O*a*2	3.16 (2)		C*c*14···C*a*12^{x}	3.47 (2)
C*c*2···O*a*2	3.40 (3)		O*c*4···C*b*13^{xii}	3.20 (2)
C*c*2···O*a*2^{xv}	3.47 (3)		O*c*6···C*b*11^{xvi}	3.14 (2)
N*c*3···O*a*2^{xv}	3.40 (3)		O*c*6···C*b*12^{xvi}	3.35 (2)
O*c*2···N*a*1	3.32 (2)		C*c*12···O*b*2^{xv}	3.34 (3)
O*c*2···C*a*2^{xv}	3.31 (3)			

Symmetry codes: (i) $x-\frac{1}{2}, -y+\frac{1}{2}, z-\frac{1}{2}$; (ii) $x+\frac{1}{2}, -y+\frac{1}{2}, z+\frac{1}{2}$; (iii) $-x, -y, -z$; (iv) $-x+1, -y, -z+1$; (v) $x+\frac{1}{2}, -y+\frac{1}{2}, z-\frac{1}{2}$; (vi) $x, y, z+1$; (vii) $x, y, z-1$; (viii) $-x, -y, -z+1$; (ix) $x-\frac{1}{2}, -y+\frac{1}{2}, z+\frac{1}{2}$; (x) $-x, -y+1, -z+1$; (xi) $-x+1, -y+1, -z+2$; (xii) $-x+1, -y, -z+1$; (xiii) $-x, -y, -z$; (xiv) $-x+1, -y+1, -z+1$; (xv) $x, y, z-1$; (xvi) $-x, -y+1, -z+2$; (xvii) $-x, -y, -z+1$.

Brückner, S. & Immirzi, A. (1997). *J. Appl. Cryst.* **30**, 207–208.
Caglioti, G., Paoletti, A. & Ricci, F. P. (1958). *Nucl. Instrum.* **3**, 223–228.
Cleverley, B. & Williams, P. P. (1959). *Tetrahedron*, **7**, 277–288.
Craven, B. M. & Vizzini, E. A. (1971). *Acta Cryst.* B**27**, 1917–1924.
Craven, B. M., Vizzini, E. A. & Rodrigues, M. M. (1969). *Acta Cryst.* B**25**, 1978–1993.
Dollase, W. A. (1986). *J. Appl. Cryst.* **19**, 267–272.
Evain, M., Deniard, P., Jouanneaux, A. & Brec, R. (1993). *J. Appl. Cryst.* **26**, 563–569.
Farrugia, L. (1997). *J. Appl. Cryst.* **30**, 565.
Favre-Nicolin, V. & Cerny, R. (2002). *J. Appl. Cryst.* **35**, 734–743.
Kempster, C. J. E. & Lipson, H. (1972). *Acta Cryst.* B**28**, 3674.
March, A. (1932). *Z. Kristallogr.* **81**, 285–297.

Mesley, R. J., Clements, R. L., Flaherty, B. & Goodhead, K. (1968). *J. Pharm. Pharmac.* **20**, 329–340.
Nakao, S., Fujii, S., Sakaki, T. & Tomita, K. (1977). *Acta Cryst.* B**33**, 1373–1378.
Rodriguez-Carvajal, J. (2001). *FullProf*, Version 1.9c. LLB, CEA/ Saclay, France.
Rodriguez-Carvajal, J. & Roisnel, T. (2004). *Mater. Sci. Forum*, **443–444**, 123–126.
Roisnel, T. & Rodriguez-Carvajal, J. (2002). *Mater. Sci. Forum*, **378–381**, 118–126.
Thompson, P., Cox, D. E. & Hastings, J. B. (1987). *J. Appl. Cryst.* **20**, 79–83.
Werner, P. E., Eriksson, L. & Westdahl, M. (1985). *J. Appl. Cryst.* **18**, 367–370.
Williams, P. P. (1973). *Acta Cryst.* B**29**, 1572–1579.
Williams, P. P. (1974). *Acta Cryst.* B**30**, 12–17.